Molecular Vision 2013; 19:2196-2208 <http://www.molvis.org/molvis/v19/2196>
Received 5 July 2013 | Accepted 5 November 2013 | Published 7 November 2013

Cataract-specific posttranslational modifications and changes in the composition of urea-soluble protein fraction from the rat lens

Lyudmila V. Yanshole,[1,2] Ivan V. Cherepanov,[1] Olga A. Snytnikova,[1,2] Vadim V. Yanshole,[1,2] Renad Z. Sagdeev,[1] Yuri P. Tsentalovich[1,2]

[1]International Tomography Center SB RAS, Novosibirsk, Russia; [2]Novosibirsk State University, Novosibirsk, Russia

Purpose: To determine age-related changes in the composition of the urea-soluble (US) protein fraction from lenses of senescence-accelerated OXYS (cataract model) and Wistar (control) rats and to establish posttranslational modifications (PTMs) occurring under enhanced oxidative stress in OXYS lenses.
Methods: The identity and the relative abundance of crystallins in the US fractions were determined using two-dimensional gel electrophoresis (2-DE) and matrix-assisted laser desorption ionization–time of flight mass spectrometry (MS). The identities and the positions of PTMs were established using MS/MS measurements.
Results: Two-dimensional gel electrophoresis maps of US protein fractions were obtained for lenses of 3-, 12-, and 62-week-old Wistar and OXYS rats, and the relative abundance of different isoforms of α-, β-, and γ-crystallins was determined. β-Crystallins were the major contributor of the US fraction in 3-week-old lenses (above 50%), γ-crystallins in 12-week-old lenses (50–60%), and in 62-week-old lenses, the contributions from all three crystallin families leveled out. The major interstrain difference was the elevated level of α-crystallins in the US fraction from 12-week-old OXYS lenses. Spots with increased relative abundance in OXYS maps were attributed to the cataract-specific spots of interest. The crystallins from these spots were subjected to MS/MS analysis, and the positions of acetylation, oxidation, deamidation, and phosphorylation were established.
Conclusions: The increased relative abundance of α-crystallins in the US fraction from 12-week-old OXYS lenses points to the fast insolubilization of α-crystallins under oxidative stress. Most of the PTMs attributed to the cataract-specific modifications also correspond to α-crystallins. These PTMs include oxidation of methionine residues, deamidation of asparagine and glutamine residues, and phosphorylation of serine and threonine residues.

The major cause of cataract development is the accumulation of posttranslational modifications (PTMs) in the lens proteins, specifically crystallins [1]. All crystallins are initially water soluble (WS). The protein turnover in the lens is very small, and PTMs in crystallins accumulate throughout the whole lifespan. PTMs can affect both the structure and functionality of proteins; they cause protein coloration, aggregation, and insolubilization. Eventually, the formation of large water-insoluble (WIS) protein aggregates leads to light scattering and lens clouding. The most common reported PTMs of crystallins are truncation, oxidation, deamidation, acetylation, phosphorylation, and glycosylation.

Previously, it was shown that C-terminal truncation of even five amino acids in the α-crystallin sequence may diminish its ability to act as chaperone [2-4]. β-Crystallins in the lens are also susceptible to N- and C-terminal cleavage, and this may affect subunit organization and higher order assembly [5-7]. The thiol-rich β- and γ-crystallins are most susceptible to oxidation; oxidation of αA- and αB-crystallins also occurs, leading to structural changes and loss of chaperone activity [1]. Deamidation is the major PTM that may lead to the insolubilization of α- and β-crystallins, changing their tertiary structure and encouraging unfolding.

It is important to note that numerous PTMs are found in both cataractous and healthy aged lenses. Cataract is so common a disease among elderly people that it is sometimes considered a part of the natural aging process. However, many people maintain clear vision up to a very old age, which suggests that there is a principal distinction between cataract and lens aging. The goal of the present work is to establish PTMs specific for cataractogenesis. It is common to divide lens proteins into the following three fractions: the WS fraction, which contains mostly intact or slightly modified proteins; the WIS urea-soluble (US) fraction representing moderately modified proteins; and the urea-insoluble fraction containing heavily damaged crystallins, whose structure is so strongly disrupted that they cannot be dissolved even in urea solution. In this work, we performed an analysis of the US protein fractions from the lenses of two rat strains—Wistar and senescence-accelerated OXYS rats.

The OXYS strain is a model of age-related cataract developed from the Wistar stock. The first signs of cataract

Correspondence to: Yuri P. Tsentalovich, International Tomography Center, 630090, Institutskaya 3a, Novosibirsk, Russia. Phone: +7-383-3303136; FAX: +7-383-3331399; email: yura@tomo.nsc.ru

in OXYS rats appear at the age of 6 weeks; by the age of 12 weeks, 90% of animals are affected by the lens opacification. For comparison, the initial signs of cataract appear in the lenses of Wistar rats after 24 weeks. The characteristic feature of OXYS rats is the excessive generation of reactive oxygen species [8], which is responsible for the accelerated aging of the animals in general, and for the early cataract onset in particular. Thus, the comparative analysis of proteomic composition of OXYS and Wistar lenses of the same age, as well as of PTMs in the lens proteins, may help to separate age-related and cataract-specific changes in the lens proteome.

In our recent paper [9], we studied the age-related changes in the composition of WS protein fraction from OXYS and Wistar lenses. It has been shown that the most pronounced age-related changes in the protein composition of the rat lens are the increase of WIS/WS ratio with aging, the fast insolubilization of γ-crystallins, and the increase of the relative abundance of αB- and βB2-crystallins in the WS protein fraction during lens growth. The major observed differences between Wistar and OXYS lenses are the faster decay of the content of γ-crystallins in OXYS lenses, and the significant decrease of unmodified αA-crystallin abundance in old OXYS lenses. These differences have been attributed to cataract-specific changes in the protein composition of the lens. In the present work, we report the analysis of the proteomic composition and PTMs of the US protein fraction from OXYS and Wistar lenses.

METHODS

Materials and reagents: Phosphate buffer tablets (PBS: [0.02 M sodium phosphate, 0.274 M sodium chloride, 0.054 M potassium chloride, pH 7.3], Biolot, Saint-Petersburg, Russia); urea and ampholytes (Bio-Lyte 3/10, Bio-Lyte 5/8); CHAPS detergent, Tris-HCl, glycine, sodium dodecyl sulphate, agarose, iodoacetamide and bovine serum albumin standard (BSA) (Bio-Rad, Hercules, CA); acrylamide (4K, Medigen, Novosibirsk, Russia); acrylamide for isoelectric focusing (IEF, Amersham Biosciences, Uppsala, Sweden); bis-acrylamide (Amresco, Solon, OH); ammonium persulphate, tetramethylethylenediamine, bromophenol blue, dithiothreitol (Helicon, Moscow, Russia); NaOH and orthophosphoric acid (Reachim, Moscow, Russia); glycerol and acetonitrile (Panreac, Barcelona, Spain); Coomassie brilliant blue R-250 and trifluoroacetic acid (Sigma, Steinheim, Germany); acetic acid (Chimreactiv, Moscow, Russia); ammonium bicarbonate (Fluka, Steinheim, Germany); sequencing grade modified trypsin (Promega, Madison, WI); Bradford reagent (Fermentas, Burlington, Ontario, Canada); and 2,5-dihydroxybenzoic acid (Bruker Daltonics, Bremen, Germany) were used as received. H_2O was deionized using an ultra pure water system (SG water/Siemens, Alpharetta, GA) to 18.2 MOhm.

Animals and lens preparation: All animals were kept and treated according to the Association for Research in Vision and Ophthalmology Statement for the Use of Animals in Ophthalmic and Vision Research. The experimental rats were housed in groups of five animals per cage (57 cm×36 cm×20 cm) and kept under standard laboratory conditions (at 22±2 °C, 60% relative humidity, natural light), provided with a standard rodent diet PK120–1 (Laboratorsnab, Russia), and given water ad libitum. Animals were sacrificed by diethyl ester asphyxiation, the eyes were extracted, and the whole lenses removed. Lenses were obtained from senescence-accelerated OXYS rats at 3, 12, and 62 weeks of age and from age-matched Wistar rats. The removed lenses were frozen in liquid nitrogen and stored at −70 °C until analysis.

Protein extraction: Each lens (with the exception of 3-week-old rat lenses) was homogenized on ice in 700 µl of 0.02 M PBS, pH 7.3, containing protease inhibitor cocktail. Since the lenses of 3-week-old rats are small, five lenses were pooled for the homogenization in the same solution. The homogenate was separated into WS and US (pellet) fractions by centrifugation at 12,000g for 50 min at 4 °C. The pellet was resuspended twice in 300 µl and 200 µl of H_2O and centrifuged at 12,000g for 30 min at 4 °C. After removing the WS proteins, the pellet was dissolved in a buffer containing 50 mM Tris, 3 mM dithiothreitol, and 8 M urea, and sonicated in the ultrasonic bath for 20 min. The volume of the buffer solution added to the pellet of 3-week-old rats was 150 µl, and 200 µl for the pellets of other ages. The dissolved samples were incubated with 20 µl of freshly prepared 10 mM iodoacetamide solution in a dark place for 30 min with occasional vortexing. The protein content in all samples was determined using Bradford reagent [10] and BSA standards following the manufacturer's protocol: 250 µl of Bradford reagent was mixed with 5 µl of sample or BSA standard solution directly in a 96-well flat-bottom plate (Greiner bio-one, Monroe, NC) and incubated for 2 minutes at room temperature. The absorption at 620 nm was measured for all samples. The total protein concentration in the sample was calculated using the calibration curve obtained for BSA standard solutions (250, 500, 750, 1000, 1500, 2000 µg/ml).

Two-dimensional gel electrophoresis and protein quantification and identification: Two-dimensional electrophoresis of US lens proteins and protein quantification and identification were performed according to the procedure described previously [9]. Briefly, IEF was performed using a "tube gel"

system: The US protein mixture was loaded onto the top of the gels in glass tubes. After the IEF stage, the gels were extruded from the tubes into the tray with buffer solution, and then placed over the 12% sodium dodecyl sulfate polyacrylamide gels (20×20 cm, thickness 1.5 mm) for the second dimension. Images of Coomassie-stained gels were obtained using a VersaDoc Imaging System (4000 MP, Bio-Rad), and calculation of the protein percentage abundances was performed with a PDQuest Advanced 2D-analysis Software 8.0.1. Protein in-gel digestion was performed with sequencing grade modified trypsin (12.5 ng/µl) in 40 mM ammonium bicarbonate for 16 h at 37 °C. Proteins from gels were identified by mass spectrometry (MS) analysis using a matrix-assisted laser desorption ionization–time of flight MALDI-TOF/TOF spectrometer Ultraflex III (Bruker Daltonics). The mass spectra of the protein tryptic digests were recorded in the reflective positive ion mode in the 500–4200 m/z range. Spectra were then analyzed using FlexAnalysis software 3.0 (Bruker Daltonics, Germany), and peptide masses were entered into the local MASCOT server 2.2.04 (Matrix Science, UK) for the "peptide mass fingerprinting" protein identification method. The MALDI-TOF identities of proteins were established by using the SwissProt_2013 database (mass accuracy: 70 ppm; one missed cleavage; variable modifications: partial methionine oxidation, protein N-terminal acetylation, asparagine and glutamine deamidation, serine and threonine phosphorylation).

Identification of posttranslational modifications: Tandem MS experiments were performed using the MALDI-TOF/TOF spectrometer Ultraflex III. The signals in MS mode that were preliminary assigned to the modified crystallin peptides were chosen for the further MS/MS analysis. The high-energy collision-induced dissociation tandem mass spectra of fragments were recorded in the positive ion mode. Fragment ions were obtained using the Bruker LIFT method (TOF/TOF). Tandem spectra were then analyzed using FlexAnalysis software. A MASCOT MS/MS search using SwissProt_2013 database was performed with a peptide mass tolerance of 70 ppm and fragment mass tolerance of 0.4 Da. A maximum of one trypsin missed cleavage was tolerated. The database search for fragment ions was performed with the selection of modifications found for the parent peptides. The peptide identification was considered conclusive only if a MASCOT ion score indicating protein identity lower than 0.05 was obtained.

Statistical analysis: All statistical calculations were carried out using the software package Statistica 6.0 (Statsoft, USA) using factor dispersion analysis (analysis of variance/multivariate analysis of variance) and the Newman-Keuls post-hoc test for comparison of group mean values.

RESULTS

Composition of the urea-soluble protein fraction: Figure 1 shows two-dimensional gel electrophoresis (2-DE) maps of the US protein fractions of 3-week-old, 12-week-old, and 62-week-old Wistar and OXYS lenses. The spots containing proteins were excised, and after the in-gel tryptic digestion, the identities of proteins were determined using MS analysis through the peptide mass fingerprinting method. Approximately 60% of spots in each gel were identified with a sequence coverage of 70–98%; the sequence coverage for the remaining 40% was about 50–70%. An example of the assignment of proteins from the US fraction of 12-week-old OXYS lens is given in Figure 2 and Table 1. The relative abundance of crystallins present in the gel was determined by the numerical integration of each spot. The values obtained for the spots attributed to the same crystallin were summarized, and the percentage abundance of each crystallin was calculated. The same procedure was performed for four gels from each age and strain; the data obtained for the same age and strain were averaged. In some gels, the spots related to γA-, γB-, and γD-crystallins overlapped; therefore, the percentage abundances of these crystallins were combined. The obtained results are presented in Figure 3.

The proteomic profiles of the young Wistar and OXYS lenses (3-week-old) were similar: β-Crystallins provided the major contribution to the US fraction (above 50%), followed by γ-crystallins (approximately 27%). The contribution of α-crystallins was relatively small (8–12%). At the age of 12 weeks, a significant growth in γ-crystallin content and a decrease of β-crystallin content was observed for both rat strains. At the same time, the relative abundance of α-crystallins in the US fraction of the Wistar lens decreased, and that of the OXYS lens increased. As a result, at this age, the γ-crystallins became the main constituents of the US protein fraction in both Wistar and OXYS lenses (50–60%), and the content of α-crystallins in the Wistar lens dropped to approximately 6%. The percentage of α-crystallins in the OXYS 12-week-old lens is almost threefold higher. Finally, in old lenses (62 weeks), the contributions from all three crystallin families level out for both strains at 22–25% for α-crystallins, 32–33% for β-crystallins, and 37–42% for γ-crystallins. In Figure 3, the crystallins whose percentage abundances in Wistar and OXYS lenses differ significantly ($p<0.05$) are marked by asterisk.

Posttranslational modifications: The comparison of 2-DE maps of the US protein fraction from Wistar and OXYS

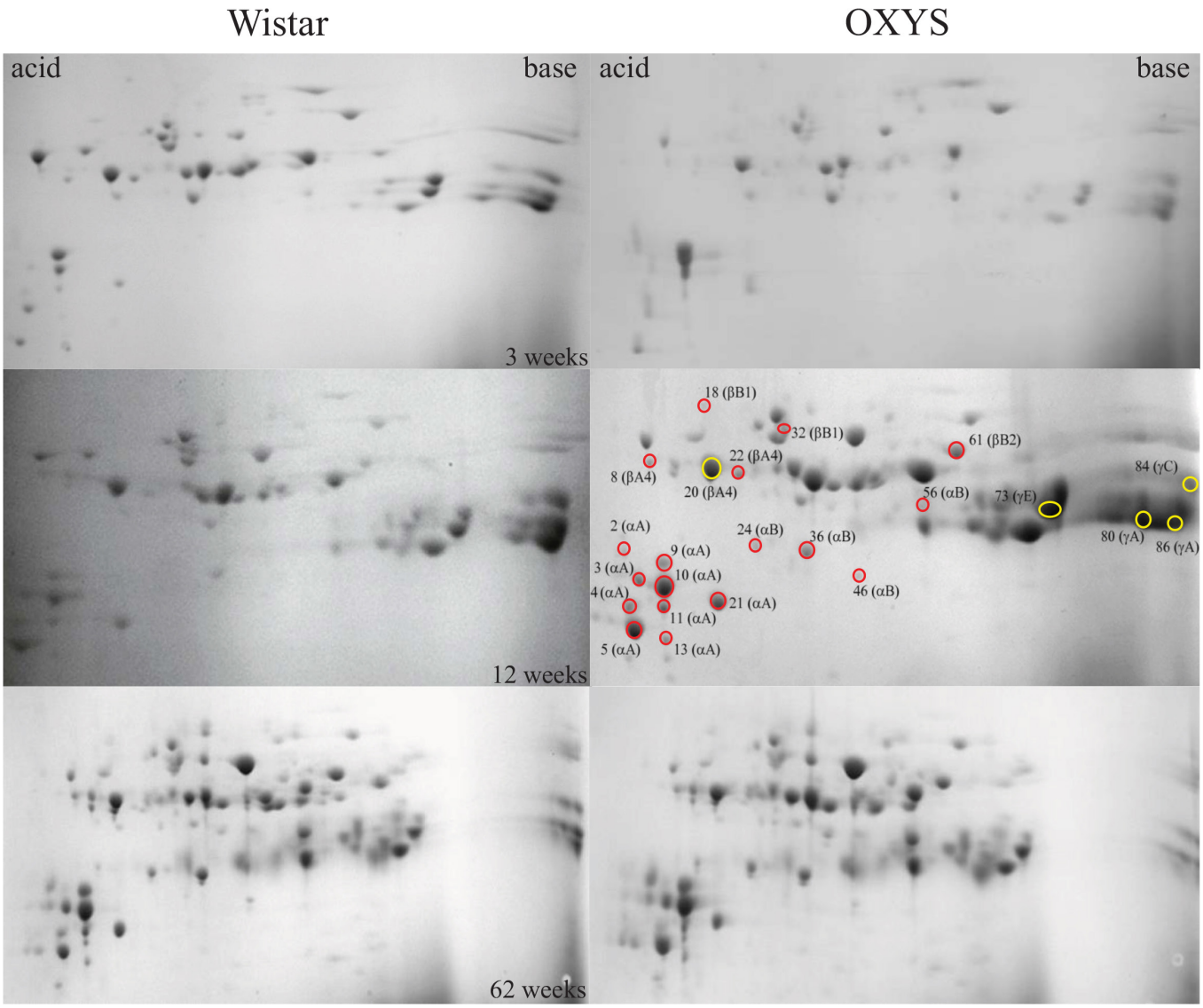

Figure 1. Two-dimensional electrophoresis maps of urea-soluble protein fractions from lenses of 3-, 12-, and 62-week-old Wistar and OXYS rats. Red circles mark cataract-specific spots of interest (SOI_{cs}; spot intensity in OXYS maps are more than 50% higher than in Wistar maps); yellow circles mark age-related spots of interest (SOI_{ar}; spot intensity in OXYS maps are more than 50% lower than in Wistar maps).

lenses of different ages (Figure 1) shows that the maps obtained for Wistar and OXYS lenses at the age of 3 weeks are very similar. This confirms that genetically, these strains are very close, and during the first 3 weeks of life, no significant difference in the proteomic composition of the lens has accumulated. The difference becomes noticeable at the age of 12 weeks: Some new spots appear in the proteomic map of the OXYS lens that are absent in the map of the Wistar lens, and some spots significantly differ in density. This difference becomes even more pronounced at the age of 62 weeks. Apparently, the observed difference should be attributed to the enhanced oxidative stress in OXYS rats, which results in the faster oxidative damage of the lens proteins. At the age of 12 weeks, most of the OXYS rats have the initial signs of cataract, while the lenses of the Wistar rats at this age are clear [11]. Therefore, we have chosen 12-week-old OXYS lenses for the detailed analysis of the oxidation-induced PTMs.

The relative abundance of each spot has been determined in the proteomic maps from four Wistar and four OXYS lenses, and the mean values have been calculated. The densities of 18 spots in the OXYS maps were more than 50% higher than those in the Wistar maps. One can presume that these spots contain proteins with PTMs formed under enhanced

Table 1. Proteins identified in the US fraction of 12-week-old OXYS rat lens.

Protein	Spot number	Protein	Spot number
αA	1–5, 9–14, 21	γA	65, 77, 80, 86
$αA_{insert}$	33, 38, 44	γB	45, 76, 79, 85
αB	17, 24, 36, 41, 46, 56	γC	78, 84
βA2	34	γD	57, 60, 63, 67, 70
βA3	29, 37, 39, 40, 43, 48, 50, 52, 55, 58	γE	66, 73
βA4	8, 15, 16, 20, 22, 23	γF	59, 64, 68, 74
βB1	7, 18, 19, 25–28, 30–32, 47, 49, 53	γN	35
βB2	42, 61	γS	54
βB3	51, 62, 69, 71, 72, 75, 81–83	Grifin	6

Spot numbers correspond to 2-DE map in Figure 2.

oxidative stress. These spots (cataract-specific spots of interest, SOI_{cs}) are marked by red circles in Figure 1. Nine of the SOI_{cs} (2–5, 9–11, 13, 21) correspond to αA-crystallin, four (24, 36, 46, 56) to αB-crystallin, two (8, 22) to βA4-crystallin, two (18, 32) to βB1-crystallin, and one (61) to βB2-crystallin. The other group of spots, one of which corresponds to βA4-crystallin (20) and four to γ-crystallins (73, 80, 84, 86), has a relative abundance in OXYS maps that is significantly lower than that in Wistar maps. The high relative abundance of these protein isoforms in the Wistar US fraction may indicate that PTMs in these crystallins correspond to the natural aging process: In the absence of excessive oxidative stress, the relative abundance of proteins with natural age-related PTMs is higher than that in the OXYS lens. We have called these spots age-related spots of interest, SOI_{ar}. In Figure 1, SOI_{ar} are marked by yellow circles. All SOI_{cs} and SOI_{ar} have been excised from the gel, and after in-gel digestion, subjected to MS/MS analysis.

It should be noted that two artificial modifications were identified in all examined crystallins. Cysteine residues were modified with propionamide and carbamidomethyl; these modifications are well known to occur during the sample preparation. Besides these two modifications, our search included oxidation of methionines (Met, M), deamidation of asparagines (Asn, N) and glutamines (Gln, Q), phosphorylation, and N-terminal acetylation. If the peptides with masses corresponding to these modifications were found, the modifications and their positions were validated with the use of MS/MS measurements.

Oxidation of methionine residues: The oxidation of methionines was revealed in all isoforms of α-crystallins subjected to MS/MS analysis. Met-1 was oxidized in all SOI_{cs}, corresponding to αA- (peptide M(Ox)DVTIQHPWFK) and αB-crystallins (peptide M(Ox)DIAIHHPWIR); moreover, the oxidation of Met-138 in αA-crystallin (peptide

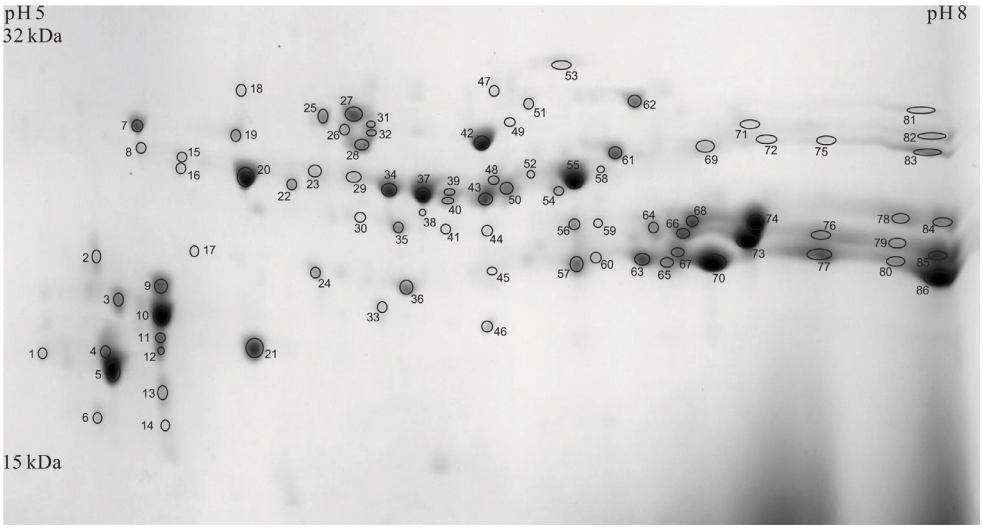

Figure 2. Two-dimensional electrophoresis map of urea-soluble lens proteins of 12-week-old OXYS rats. The spot assignment is presented in Table 1.

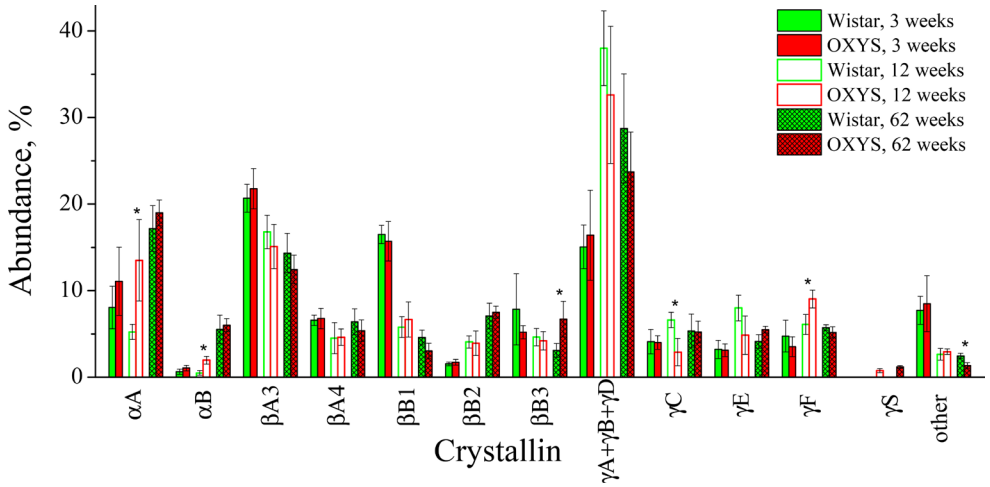

Figure 3. Relative abundances of urea-soluble crystallins extracted from lenses of Wistar and OXYS rats. Solid bars show the values for 3-week-old animals, open bars for 12-week-old animals, and hatched bars for 62-week-old animals. The error bars show standard deviations. The asterisk indicates statistically significant ($p<0.05$) interstrain differences.

LPSNVDQSALSCSLSADGM(Ox)LTFSGPK) was observed in spots 3, 4, 9, and 10 (Table 2), as well as the oxidation of Met-68 in αB-crystallin (spot 36). An example of the MS/MS confirmation of the modification position is shown in Figure 4. The MS/MS spectrum was obtained for a peptide derived from the tryptic digestion of the αA-crystallin from spot 5. The parent ion with m/z 1459.7 corresponding to the N-acetylated and singly oxidized $αA_{1–11}$ peptide MDVTIQHPWFK was isolated and fragmented using the collision-induced dissociation technique. The ion with the most intensive peak in the spectrum (m/z 1395.8) was formed by the loss of methyl sulfenic acid (CH_3SOH, 64 Da) from the parent ion, which testifies to the presence of oxidized methionine in the peptide [12,13]. The obtained y-type of fragment ions describes the peptide fragmentation from the carboxyl to the N-terminus of the peptide. It is presented with signals $y_2–y_{10}$ and a parent ion. The amino acid sequence of $αA_{1–11}$ peptide with acetylated and oxidized N-terminal methionine and the corresponding fragment ions are shown in the chart above the spectrum. The y_{10} ion with m/z 1270.7 corresponds to the $αA_{1–11}$ peptide without the acetylated and oxidized N-terminal methionine (loss of 189 Da). The signals from $y_2–y_8$ refer to the $αA_{1–11}$ peptide fragments cleaved by one amino acid from the C-terminus of the previous fragment.

The b-type of ions ($b_1–b_{10}$), showing the peptide fragments from the amino to carboxyl terminus, is also present in the MS/MS spectrum. Due to the N-terminal modifications, the masses of all b-ions are higher than the predicted masses for the unmodified fragments by 58 Da. Three a-type ions were also found in the spectrum; however, since the signals from these species are weak, and only few a-ions were observed, these fragments were not included in the interpretation of MS/MS spectra. A similar identification of the N-terminal methionine oxidation and acetylation of αA-crystallin from the mouse lens has recently been published [14]. It is often difficult to determine whether the methionine oxidation occurred in vivo or it was artificially introduced during the sample preparation. However, the presence of unmodified Met-138 in spots 2, 5, 11, and 21 indicates that the reported methionine oxidation is a real PTM and not an artifact. This conclusion is supported by previous reports [14-17] stating that the oxidation of Met-1 and Met-138 in αA-crystallin and of Met-1 and Met-68 in αB-crystallin takes place in the tissue.

Two SOI_{cr} corresponding to βB1-crystallin also contained oxidized methionines: Met-135 and Met-162 in spots 18 and 32, and Met-224 in spot 18. The positions of the modifications were also confirmed by MS/MS analysis. It has been reported that the oxidized fragments of β-crystallins inhibit the ability of α-crystallin to prevent crystallin precipitation caused by heat denaturation, and these structural changes may lead to strong interactions among β-crystallins producing light-scattering aggregates [18,19]. Thus, the observed oxidation of β-crystallins may be one of the reasons for the protein precipitation and transition into the WIS state.

The oxidized methionines were also found in the analyzed SOI_{ar}, specifically in βA4- (Met-132 in spot 20), γA- (Met-136 and Met-160 in spots 80, 86, and Met-124 in spot 86), γC- (Met-102 in spot 84), and γE- (Met-44, Met-102 and Met-160 in spot 73) crystallins. The enhanced relative abundance of oxidized γ-crystallins in 12-week-old Wistar lenses in comparison with OXYS ones testifies that the oxidation of γ-crystallins leading to their insolubilization is a part of the natural aging process.

N-terminal acetylation: The acetylation of N-terminus (the mass shift +42 Da) was found in all SOIs corresponding to

Table 2. Post-translational modifications identified for proteins in SOI_{CS} and SOI_{AR} for 12-week-old OXYS lens.

Spot N° (Crystallin)	Sequence coverage, %	Abundance, %		Modification			
		Wistar	OXYS	Oxidation (M)	Acetylation (N-term)	Deamidation (N, Q)	Phosphory-lation (S, T)
Cataract-specific spots of interest (SOIcs)							
2 (αA)	59	ND	0.3±0.3	M1	M1		T4
3 (αA)	87	0.17±0.09	0.83±0.16	M1, M138	M1		T4
4 (αA)	89	0.13±0.14	0.61±0.24	M1, M138	M1		T4
5 (αA)	89	1.26±0.37	3.06±1.28	M1	M1	N123	T4
9 (αA)	82	0.46±0.35	1.32±0.54	M1, M138	M1	N123, Q126	T4
10 (αA)	71	1.29±0.37	3.58±0.86	M1, M138	M1		T4
11 (αA)	78	0.34±0.17	0.78±0.39	M1	M1	N123, Q126	T4
13 (αA)	48	ND	0.30±0.07	M1	M1		T4
21 (αA)	87	0.84±0.25	1.59±0.57	M1	M1		T4
24 (αB)	65	ND	0.30±0.14	M1	M1		S19
36 (αB)	73	0.49±0.27	0.85±0.13	M1, M68	M1	N146	
46 (αB)	65	ND	0.19±0.05	M1	M1	N146	S19
56 (αB)	70	ND	0.52±0.13	M1	M1	N146	
8 (βA4)	98	ND	0.23±0.05			Q112, N114, Q187, Q189	
22 (βA4)	96	ND	0.66±0.37			Q112, N114	
18 (βB1)	72	ND	0.13±0.07	M135, M162, M224			
32 (βB1)	67	ND	0.91±0.30	M135, M162			
61 (βB2)	93	0.86±0.33	1.71±0.71			N174, Q185	
Age-related spots of interest (SOIar)							
20 (βA4)	91	4.51±1.80	2.90±0.86	M132		Q63, Q65, Q66, Q112, N114, Q187, Q189	
80 (γA)	63	4.61±2.51	2.17±1.39	M136, M160			
86 (γA)	66	11.5±2.61	5.17±1.11	M136, M160, M124			
84 (γC)	58	4.32±1.57	1.93±0.96	M102			
73 (γE)	58	6.89±1.67	3.65±1.98	M44, M102, M160		N50, N161	

ND (not detected) – protein spots are not found in the 12-week-old Wistar 2-DE maps.

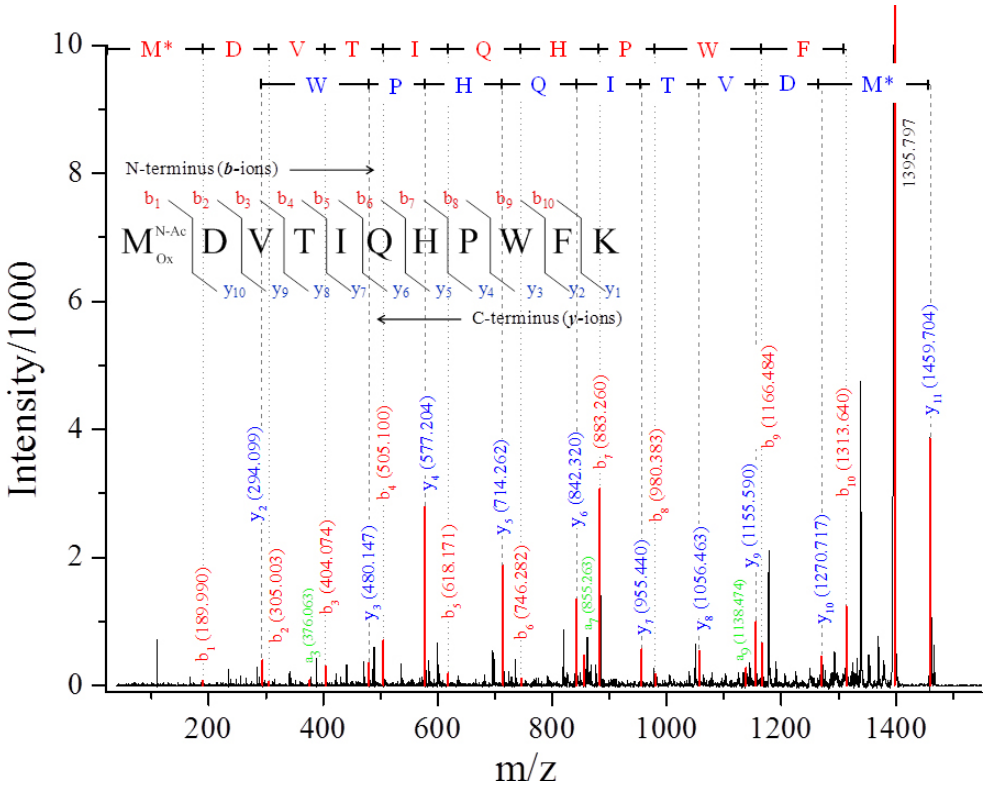

Figure 4. Tandem mass spectrum of the N-terminal peptide M*DVTIQHPWFK of αA-crystallin from spot 5 (m/z 1459.7). M* corresponds to acetylated and oxidized methionine. The signals in the spectrum are assigned as follows: y- (blue), b- (red), and a- (green) ions. The identified fragments are marked above the signals. The diagram of y- and b-ion formation is presented in the chart above the spectrum.

αA-crystallin (Table 2), both with and without oxidation of the N-terminal methionine. At the same time, this modification was not revealed in other SOIs. In fact, N-terminal peptides were not observed in any SOI corresponding to βA4-, βB1-, βB2-, and γ-crystallins. The absence of the N-terminal peptide in the mass spectra of γ-crystallins could be attributed to the fact that the terminal peptide MGK has a low m/z value, so its signal might overlap with the signals from 2,5-dihydroxybenzoic acid matrix used in MALDI experiments. The N-terminal peptides of β-crystallins are significantly longer, and their absence probably indicates N-terminal truncation of the proteins in SOIs.

Deamidation of asparagine and glutamine residues: In our research, nine spots with αA-crystallin from the OXYS rat lens were analyzed, and deamidation was detected only in three spots—at Asn-123 (spots 5, 9, 11) and Gln-126 (spots 9, 11). In αB-crystallin, the deamidation was found at Asn-146 (spots 36, 46, 56).

Deamidated proteins were also found in SOI_{ar}. Among the γ-crystallins analyzed in the present work, only γE-crystallin from spot 73 contained two deamidated asparagines—Asn-50 and Asn-161. In other γ-crystallins inspected in this work, no deamidation sites were detected. It should be noted that the sequence coverage for the examined γA-, γC- and γE-crystallins after MASCOT search was approximately 60%, which means that there is a probability of missed deamidation sites.

A high level of deamidation was observed in βA4-crystallin (SOI_{ar} 20). The deamidation sites were glutamines at the 63, 65, 66, 112, 187, and 189 positions and asparagine at the 114 position. Some of these modifications were also found in SOI_{cs}, corresponding to βA4-crystallin: Deamidation of Gln-112 and Asn-114 was found in spots 8 and 22, while deamidation of Gln-187 and Gln-189 only in spot 22. Thus, the deamidation of asparagines and glutamines was observed in both SOI_{cr} and SOI_{ar} corresponding to βA4-crystallin, so it is difficult to estimate the role of this modification in cataractogenesis. Our results can be compared with previous data on human crystallins [18,20]. The homology of the amino acid sequences of the human and rat βA4-crystallin is about 91% (Uniprot), so it is correct to make such a comparison. In human βA4-crystallin, deamidation was found for glutamines Gln-63, Gln-65, and Gln-66 and asparagines Asn-83 and Asn-114. To the best of our knowledge, this work represents the first time the deamidation of asparagines in the 187 and 189 positions in βA4-crystallin from the rat lens has been identified.

Phosphorylation of serine and threonine residues: In the present work, phosphorylated peptides were found in all SOI_{cs} corresponding to αA-crystallin (spots 2–5, 9–11, 13, and 21) and in two SOI_{cs} corresponding to αB-crystallin (spots 24 and 46). The phosphorylation of Thr-4 was found in the N-terminal peptide 1–11 (MDVTIQHPWFK) from αA-crystallin. The obtained result is in a good agreement with the previous data on the phosphorylation sites in αA-crystallin from the rat and mouse lenses [14,17,20,21]. It was noticed that the phosphorylation causes a shift of the spot position to the acidic region [14,22,23]. An acidic shift for the investigated αA-crystallin isoforms was observed in the 2-DE maps obtained in the present work (Figure 1), which also confirms the presence of phosphorylated residues in αA-crystallin.

DISCUSSION

In young lenses, crystallins are mostly present in the WS state. For example, the WIS fraction in the 3-week-old lens accounts to only 10% of the total protein content [9]. Oxidative stress causes PTMs, which may result in the protein insolubilization. Therefore, the WIS/WS ratio increases with age to approximately 0.4 at 12 weeks and to 0.8 at 62 weeks [9]. The age-related variations of the US fraction content are determined by three major factors, specifically the susceptibility of crystallins to PTMs that are able to affect their solubility, the rate of the crystallin's final degradation, and the synthesis of new crystallins inside the lens during the lifespan. Previous studies have revealed that the expression of γ-crystallins drops within the first few months after birth [24,25], and these proteins undergo insolubilization faster than α- and β-crystallins [9,26-28]. These features explain the nonmonotonic changes of the γ-crystallin content in the US fraction of the rat lens. During the first 12 weeks, a significant amount of the γ-crystallins undergoes PTMs and passes from the WS to US state, which leads to the increase of the γ-crystallin content in the US fraction of 12-week-old lenses. At older ages, the synthesis of new γ-crystallins in the lens outer cortex and epithelial layer stops [29,30], and after one year, the content of γ-crystallins in the WS fraction is almost completely depleted [9]. During the period between 12 weeks and 62 weeks, the final degradation of γ-crystallins occurs, so that at the age of 62 weeks, the percentage of γ-crystallins in the US fraction is lower than that at 12 weeks.

It is interesting to note that γS-crystallin was found in US fractions from 12-week-old and 62-week-old OXYS lenses, but not in Wistar lenses. This finding correlates with the recent paper by Wang et al. [22], where γS-crystallin spot was observed in the US fraction from lenses of naphthalene-treated rats, but not from lenses of normal rats. This gives strong evidence that the insolubilization of γS-crystallin occurs only under excessive oxidative stress.

In contrast to γ-crystallins, the production of both αA- and αB-crystallins in the rat lens is active even at the age of one year [24,25]. α-Crystallins are able to bind partially unfolded proteins, preventing their precipitation [20,26]. The chaperone activity of α-crystallins plays an important role in maintaining the homogeneous distribution of crystallins inside the lens fiber cells, delaying the formation of large insoluble protein aggregates and the lens opacification. Therefore, the large difference in α-crystallin content between Wistar and OXYS 12-week-old lenses can be attributed to two factors. First, the oxidation of proteins in OXYS lenses proceeds faster than that in Wistar lenses [8,9,11]. The characteristic feature of OXYS rats is the enhanced generation of reactive oxygen species [8], which is responsible for the early cataract onset. Oxidative damage may cause crystallin insolubilization and precipitation; α-crystallins prevent protein precipitation through the formation of WS aggregates with the damaged crystallins.

Under further oxidation or other PTMs, these aggregates grow in size and lose their solubility, so the enhanced oxidative stress in OXYS lenses might lead to the increased level of α-crystallins in the US protein fraction. Another explanation is the compensatory response to the oxidative stress, which causes the enhanced expression of α-crystallins. The enhanced production of α-crystallins in OXYS lenses would result in the increase of their levels both in the WS and US fractions. This explanation is supported by the previously obtained data: The enhanced expression of α-crystallins and the increased level of αA-crystallin in the WS fraction from lenses of 12-week-old OXYS rats [9] and dexamethasone-treated rats [31] have recently been reported. The increase of the α-crystallin level in the US protein fraction was also reported for rats with dexamethasone-induced cataract [22].

Among all β-crystallins, the percentage of only βB2-crystallin in the US fraction monotonously grows with age (Figure 3). βB2-Crystallin is one of the most long-expressed crystallins [32]; its expression starts only in the postnatal period [25,33], and the amount of its mRNA in the 1-year-old rat lens is comparable to that in the 1-month-old lens [25]. The increase of βB2-crystallin abundance also points to the high stability of this protein: It withstands the final degradation longer than other crystallins. Thus, the long production and the high stability of βB2-crystallin lead to its accumulation in both WS [9] and US protein fractions.

Among the PTMs studied in this work, N-terminal acetylation found for α-crystallin is unlikely to be related to the

lens aging and cataractogenesis. This modification protects proteins against proteolytic degradation by extracellular (aminopeptidases) or intracellular (cathepsin C) peptidases that are directed against certain free N-terminal residues [34,35]. In recent work [14], it was found that all isoforms of αA-crystallin in the mouse lenses of different ages, including embryos, are N-terminally acetylated. Similarly, N-terminal acetylation was found in all α-crystallins from lenses of both normal and naphthalene-treated rats [17]. It is very likely that the N-terminal acetylation of αA-crystallin occurs during or immediately after protein expression.

Three other types of PTM—oxidation, deamidation, and phosphorylation—develop during the lifespan. Protein oxidation is often considered the key process leading to cataract development [36]. The most common amino acid that was found oxidized in the crystallin sequences is methionine residue. The increased level of oxidized methionine residue correlates with the enhanced surface hydrophobicity of proteins and causes conformational changes [37]. The oxidation of αA- and αB-crystallins has been shown to lead to structural changes and loss of chaperone activity [38]. A direct link between the N-terminal methionine oxidation and the cataract formation has been proposed in previous work [16]. Thus, the oxidation of methionines in proteins found in SOI_{cr} can be attributed to the following cataract-related modifications: Met-1 and Met-138 in αA- crystallin; Met-1 and Met-68 in αB-crystallin; and Met-135, Met-162, and Met-224 in βB1-crystallin.

Deamidation is one of the major modifications in the lens; its level significantly increases in aged and cataractous lenses [39]. Deamidation introduces a negative charge to the protein at physiological pH; it also may cause isomerization [40]. The deamidation of asparagine residues converts them into a mixture of isoaspartate and aspartate. Recently, it has been shown that deamidated sites may be found in all crystallins, but β-crystallins are particularly susceptible to this modification [18,39]. The deamidation of β-crystallins can destabilize its dimers and disrupt their function in oligomer formation in the lens [41,42]. It has also been observed that several deamidation sites are more abundant in the WIS protein fraction than in the WS one [39,43], which suggests the structural instability of the modified proteins and the connection between deamidation and insolubilization. It is important to note that the intensities of α-crystallin spots with deamidated asparagines and glutamines in the OXYS maps are significantly higher than that in the Wistar maps; moreover, some of these spots (5, 36) are among the densest spots corresponding to α-crystallins. Very likely, the deamidation of Asn-123 in αA-crystallin and Asn-146 in αB-crystallin are the cataract-specific modifications proceeding under oxidative stress.

The deamidation of Asn-50 and Asn-161 in γE-crystallin found in the present work agrees with the data on deamidation of the human γD-crystallin [39] (the homology between the human γD-crystallin and the rat γE-crystallin is approximately 80%), for which deamidation of asparagines at the 50 and 161 positions and of glutamines at the 67 and 68 positions [39] has been reported. Our data show that in 12-week-old rat lenses, the deamidation occurs for asparagines and not for glutamines in γE-crystallin. This finding is in a good agreement with the previous reports that the deamidation of glutamine residues proceeds with much lower rate than that of asparagines [44].

Phosphorylation of serine (Ser, S), threonine (Thr, T), and tyrosine (Tyr, Y) residues proceeds by the transfer of phosphate group from adenosine triphosphate (ATP) catalyzed by kinases. The list of lens crystallins undergoing phosphorylation is summarized by Sharma and Santhoshkumar [20]. The most vulnerable to this modification are α-crystallins. The influence of phosphorylation on the chaperone activity of αA-crystallin is unclear: Some published data speak in favor of an enhancing effect of phosphorylation on the chaperone activity [45], while in the work of Wang et al. [46], no effect was found. It has been suggested that phosphorylation causes disassembling of α-crystallin multimers to tetramers [47], which leads to the reduction of their chaperone activity [47,48].

The most likely sites of bovine and rat αB-crystallin phosphorylation are serine residues at 19, 45, and 59 positions [21,48]. Similar phosphorylation sites have also been found in the human lenses [49,50]. It was shown that the chaperone activity of monophosphorylated αB-crystallin from bovine lenses decreases by about 30% [48]. In the present work, the phosphorylation in αB-crystallin was found in peptide 12–22 (RPFFPFHSPSR, spots 24, 46). This peptide contains two serine residues which may be phosphorylated; from our data, we could not unambiguously identify the phosphorylation site. Therefore, the assignment of the phosphorylation position at Ser-19 was made based on the literature data [21,48,51]. It is important to note that spots 24 and 36 with phosphorylated isoforms of αB-crystallin are absent in the Wistar proteome. Thus, the phosphorylation of Ser-19 in αB-crystallin can be attributed to the cataract-specific modifications.

In conclusion, the analysis of US protein fractions from Wistar and OXYS lenses demonstrates distinct interstrain differences in the age-related changes of the lens proteomic composition. The most significant difference is the elevated level of α-crystallins in US fraction from 12-week-old OXYS

lenses. This effect should be attributed either to the faster insolubilization of α-crystallins under oxidative stress, or to the enhanced expression of α-crystallins in OXYS lenses. Our study revealed that some spots in the 2-DE maps of US protein fraction from the OXYS lens are significantly more intensive than those in maps from the Wistar lens of the same age. The MS analysis of these spots shows the following PTMs: oxidation of methionine residues in most crystallins, N-terminal acetylation and phosphorylation of αA- and αB-crystallins, and deamidation of asparagine and glutamine residues in αA-, αB-, βA4-, and βB2-crystallins. Some of these modifications, such as oxidation, phosphorylation, and deamidation found in α-crystallins, very likely correspond to the cataract-specific modifications proceeding under oxidative stress.

ACKNOWLEDGMENTS

This work was supported by RFBR (Projects 11–04–00143, 11–03–00296 and 12–04–31244), the Division of Chemistry of RAS, the Government of the Russian Federation (grants 11.G34.31.0045 and 8094), and the President of the Russian Federation (grant NSh-2429.2012.3).

REFERENCES

1. Michael R, Bron AJ. The ageing lens and cataract: a model of normal and pathological ageing. Philos Trans R Soc Lond B Biol Sci 2011; 366:1278-92. [PMID: 21402586].
2. Kelley MJ, David LL, Iwasaki N, Wright J, Shearer TR. α-Crystallin chaperone activity is reduced by calpain II *in vitro* and an selenite cataract. J Biol Chem 1993; 268:18844-9. [PMID: 8395520].
3. Ueda Y, Fukiage C, Shih M, Shearer TR, David LL. Mass measurements of C-terminally truncated α-crystallin from two-dimensional gels identify Lp82 as a major endopeptidase in rat lens. Mol Cell Proteomics 2002; 1:357-65. [PMID: 12118077].
4. Nakamura Y, Fukiage C, Shih M, Ma H, David LL, Azuma M, Shearer TR. Contribution of calpain Lp82-induced proteolysis to experimental cataractogenesis in mice. Invest Ophthalmol Vis Sci 2000; 41:1460-6. [PMID: 10798663].
5. David LL, Shearer TR, Shih M. Sequence analysis of lens β-crystallins suggests involvement of calpain in cataract formation. J Biol Chem 1993; 268:1937-40. [PMID: 8420967].
6. David LL, Lampi KJ, Lund AL, Smith JB. The sequence of human βB1-crystallin cDNA allows mass spectrometric detection of βB1 protein missing portions of its N-terminal extension. J Biol Chem 1996; 271:4273-9. [PMID: 8626774].
7. David LL, Shearer TR. β-Crystallins insolubilized by calpain II *in vitro* contain cleavage sites similar to β-crystallins insolubilized during cataract. FEBS Lett 1993; 324:265-70. [PMID: 8405363].
8. Marsili S, Salganik RI, Albright CD, Freel CD, Johnsen S, Peiffer RL, Costello M. Cataract formation in a strain of rats selected for high oxidative stress. Exp Eye Res 2004; 79:595-12. [PMID: 15500819].
9. Kopylova LV, Cherepanov IV, Snytnikova OA, Rumyantseva YV, Kolosova NG, Tsentalovich YP, Sagdeev RZ. Age-related changes in the water-soluble lens protein composition of Wistar and accelerated-senescence OXYS rats. Mol Vis 2011; 17:1457-67. [PMID: 21677790].
10. Bradford MM. A rapid and sensitive method for the quantitation of microgram quantities of protein utilizing the principle of protein-dye binding. Anal Biochem 1976; 72:248-54. [PMID: 942051].
11. Rumyantseva YuV, Fursova AZh, Fedoseeva LA, Kolosova NG. Changes in physicochemical parameters and α-crystallin expression in the lens during cataract development in OXYS rats. Biochemistry (Mosc) 2008; 73:1176-82. [PMID: 19120020].
12. Jagannadham MV. Identifying the sequence and distinguishing the oxidized-methionine from phenylalanine peptides by MALDI TOF/TOF mass spectrometry in an antarctic bacterium *Pseudomonas Syringae*. Proteomics Insights 2009; 2:27-31. .
13. Guan Z, Yates NA, Bakhtiar R. Detection and characterization of methionine oxidation in peptides by collision-induced dissociation and electron capture dissociation. J Am Soc Mass Spectrom 2003; 14:605-13. [PMID: 12781462].
14. Schaefer H, Chamrad DC, Herrmann M, Stuwe J, Becker G, Klose J, Blueggel M, Meyer HE, Marcus K. Study of post-translational modifications in lenticular αA-Crystallin of mice using proteomic analysis techniques. Biochim Biophys Acta 2006; 1764:1948-62. .
15. Hanson SRA, Hasan A, Smith DL, Smith JB. The major *in vivo* modifications of the human water-insoluble lens crystallins are disulfide bonds, deamidation, methionine oxidation and backbone cleavage. Exp Eye Res 2000; 71:195-207. [PMID: 10930324].
16. Fujii N, Takeuchi N, Fujii N, Tezuka T, Kuge K, Takata T, Kamei A, Saito T. Comparison of post-translational modifications of αA-crystallin from normal and hereditary cataract rats. Amino Acids 2004; 26:147-52. [PMID: 15042443].
17. Chen Y, Yi L, Yan GQ, Jang YX, Fang YW, Wu XH, Zhou XW, Wei LM. Decreased chaperone activity of α-crystallins in naphthalene-induced cataract possibly results from C-terminal truncation. J Int Med Res 2010; 38:1016-28. [PMID: 20819438].
18. Zhang Z, Smith DL, Smith JB. Human β-crystallins modified by backbone cleavage, deamidation and oxidation are prone to associate. Exp Eye Res 2003; 77:259-72. [PMID: 12907158].
19. Udupa EG, Sharma KK. Effect of oxidized βB3-crystallin peptide on lens βL-crystallin: interaction with βB2-crystallin. Invest Ophthalmol Vis Sci 2005; 46:2514-21. [PMID: 15980243].

20. Sharma KK, Santhoshkumar P. Lens aging: Effects of crystallins. Biochim Biophys Acta 2009; 1790:1095-108. [PMID: 19463898].

21. Wang K, Gawiniowicz MA, Spector A. The effect of stress on the pattern of phosphorylation of αA and αB crystallin in the rat lens. Exp Eye Res 2000; 71:385-93. [PMID: 10995559].

22. Wang L, Liu D, Liu P, Yu Y. Proteomics analysis of water insoluble-urea soluble crystallins from normal and dexamethasone exposed lens. Mol Vis 2011; 17:3423-36. [PMID: 22219638].

23. Marcus K, Moebius J, Meyer HE. Differential analysis of phosphorylated proteins in resting and thrombin-stimulated human platelets. Anal Bioanal Chem 2003; 376:973-93. [PMID: 12904942].

24. van Leen RW, van Roozendaal KE, Lubsen NH, Schoenmakers JG. Differential expression of crystallin genes during development of the rat eye lens. Dev Biol 1987; 120:457-64. [PMID: 3030857].

25. Aarts HJ, Lubsen NH, Schoenmakers JGG. Crystallin gene expression during rat lens development. Eur J Biochem 1989; 183:31-6. [PMID: 2753045].

26. Swamy MS, Abraham EC. Lens protein composition, glycation and high molecular weight aggregation in aging rats. Invest Ophthalmol Vis Sci 1987; 28:1693-701. [PMID: 3654142].

27. Ranjan M, Nayak S, Rao BS. Immunochemical detection of glycated β- and γ-crystallins in lens and their circulating autoantibodies (IgG) in streptozocin induced diabetic rat. Mol Vis 2006; 12:1077-85. [PMID: 17093392].

28. Bindels JG, Bours J, Hoenders HJ. Age-dependent variations in the distribution of rat lens water-soluble crystallins. Size fractionation and molecular weight determination. Mech Ageing Dev 1983; 21:1-13. [PMID: 6865495].

29. Voorter CE, De Haard-Hoekman WA, Hermans MM, Bloemendal H, De Jong WW. Differential synthesis of crystallins in the developing rat eye lens. Exp Eye Res 1990; 50:429-37. [PMID: 2338125].

30. Siezen RJ, Wu E, Kaplan ED, Thomson JA, Benedek GB. Rat lens γ-crystallins. Characterization of the six gene products and their spatial and temporal distribution resulting from differential synthesis. J Mol Biol 1988; 199:475-90. [PMID: 3351938].

31. Wang L, Zhao WC, Yin XL, Ge JY, Bu ZG, Ge HY, Meng QF, Liu P. Lens proteomics: analysis of rat crystallins when lenses are exposed to dexamethasone. Mol Biosyst 2012; 8:888-901. [PMID: 22269969].

32. Zhang J, Li J, Huang C, Xue L, Peng Y, Fu Q, Gao L, Zhang J, Li W. Targeted knockout of the mouse βB2-crystallin gene (Crybb2) induces age-related cataract. Invest Ophthalmol Vis Sci 2008; 49:5476-83. [PMID: 18719080].

33. Ueda Y, Duncan MK, David LL. Lens proteomics: the accumulation of crystalline modifications in the mouse lens with age. Invest Ophthalmol Vis Sci 2002; 43:205-15. [PMID: 11773033].

34. Jörnvall H. Acetylation of protein N-terminal amino groups structural observations on α-amino acetylated proteins. J Theor Biol 1975; 55:1-12. [PMID: 1207150].

35. Driessen HP, Ramaekers FC, Vree Egberts WT, Dodemont HJ, de Jong WW, Tesser GI, Bloemendal H. The function of N-α-acetylation of the eye-lens crystallins. Eur J Biochem 1983; 136:403-6. [PMID: 6628390].

36. Truscott RJW. Age–related nuclear cataract – oxidation is the key. Exp Eye Res 2005; 80:709-25. [PMID: 15862178].

37. Chao CC, Ma YS, Stadtman ER. Modification of protein surface hydrophobicity and methionine oxidation by oxidative systems. Proc Natl Acad Sci USA 1997; 94:2969-74. [PMID: 9096330].

38. Brennan LA, Lee W, Giblin FJ, David LL, Kantorow M. Methionine sulfoxide reductase A (MsrA) restores α-crystallin chaperone activity lost upon methionine oxidation. Biochim Biophys Acta 2009; 1790:1665-72. [PMID: 19733220].

39. Wilmarth PA, Tanner S, Dasari S, Nagalla SR, Riviere MA, Bafna V, Pevzner PA, David LL. Age-related changes in human crystallins determined from comparative analysis of posttranslational modifications in young and aged lens: does deamidation contribute to crystallin insolubility. J Proteome Res 2006; 5:2554-66. [PMID: 17022627].

40. Robinson NE, Robinson AB. Prediction of primary structure deamidation rates of asparaginyl and glutaminyl peptides through steric and catalytic effects. J Pept Res 2004; 63:437-48. [PMID: 15140161].

41. Weintraub SJ, Deverman BE. Chronoregulation by asparagine deamidation. Sci STKE 2007; 2007:1-6. [PMID: 17957089].

42. Lampi KJ, Amyx KK, Ahmann P, Steel EA. Deamidation in human lens βB2-crystallin destabilizes the dimer. Biochem 2006; 45:3146-53. .

43. Hains PG, Truscott RJW. Post-translational modifications in the nuclear region of young, aged, and cataract human lenses. J Proteome Res 2007; 6:3935-43. [PMID: 17824632].

44. Joshi AB, Kirsch LE. The relative rates of glutamine and asparagine deamidation in glucagon fragment 22–29 under acidic conditions. J Pharm Sci 2002; 91:2331-45. [PMID: 12379918].

45. van Boekel MA, Hoogakker SE, Harding JJ, de Jong WW. The influence of some post-translational modifications on the chaperone-like activity of α-crystallin. Ophthalmic Res 1996; 28:32-8. [PMID: 8727961].

46. Wang K, Ma W, Spector A. Phosphorylation of α-crystallin in rat lenses is stimulated by H_2O_2 but phosphorylation has no effect on chaperone activity. Exp Eye Res 1995; 61:115-24. [PMID: 7556464].

47. MacRae TH. Structure and function of small heat shock/α-crystallin proteins: established concepts and emerging ideas. Cell Mol Life Sci 2000; 57:899-913. [PMID: 10950306].

48. Kamei A, Hamaguchi T, Matsuura N, Masuda K. Does post-translational modification influence chaperone-like activity of α-crystallin? I. Study on phosphorylation. Biol Pharm Bull 2001; 24:96-9. [PMID: 11201254].

49. Takemoto LJ. Differential phosphorylation of αA-crystallin in human lens of different age. Exp Eye Res 1996; 62:499-504. [PMID: 8759518].

50. MacCoss MJ, McDonald WH, Saraf A, Sadykov R, Clark JM, Tasto JJ, Gould KL, Wolters D, Washburn M, Weiss A, Clark JI, Yates JR. Shotgun identification of protein modifications from protein complexes and lens tissue. Proc Natl Acad Sci USA 2002; 99:7900-5. [PMID: 12060738].

51. Ito H, Iida K, Kamei K, Iwamoto I, Inaguma Y, Kato K. Alpha B-crystallin in the rat lens is phosphorylated at an early post-natal age. FEBS Lett 1999; 446:269-72. [PMID: 10100856].

Articles are provided courtesy of Emory University and the Zhongshan Ophthalmic Center, Sun Yat-sen University, P.R. China. The print version of this article was created on 7 November 2013. This reflects all typographical corrections and errata to the article through that date. Details of any changes may be found in the online version of the article.